HALOETHANE REACTIONS OVER THE CHROMIA Cr_2O_3 $(10\bar{1}2)$ SURFACE

By

Qiang Ma

Thesis submitted to the faculty of the
Virginia Polytechnic Institute and State University
In partial fulfillment of the requirements for the degree of
Master of Science

in

Chemical Engineering

Dr. David F. Cox (Chairman)

Dr. Richey M. Davis

Dr. S. Ted. Oyama

August 11, 2005

Blacksburg, VA

Key Words: metal oxide, chromium (III) oxide, hydrogenation, dehydrogenation, haloethane, ethyl iodide, ethyl chloride, dissociation

HALOETHANE REACTIONS OVER THE CHROMIA Cr_2O_3 $(10\bar{1}2)$ SURFACE

by

Qiang Ma

(Abstract)

Ethyl iodide and ethyl chloride have been used as reactants to produce ethyl fragments on the stoichiometric α-Cr_2O_3 $(10\bar{1}2)$ surface by means of thermal dissociation. Ethyl iodide is dissociated giving iodine adatoms and ethyl fragments bound to surface Cr cation sites, while ethyl chloride is dissociated giving chlorine adatoms and ethyl fragments. No oxygenated products are observed in thermal desorption, suggesting the 3-coordinate lattice oxygen on the stoichiometric α-Cr_2O_3 $(10\bar{1}2)$ surface is very stable, and no nucleophilic attack occurs at the carbon atoms on surface ethyl fragments.

For both reactants, the only reaction products observed are ethylene gas (CH_2=CH_2), ethane gas (CH_3-CH_3), hydrogen gas (H_2) and halogen adatoms (Cl_{ads} or I_{ads}). In thermal desorption experiments, all the gas phase products from ethyl chloride are produced in a reaction-limited, high temperature desorption feature attributed to a rate limiting β-hydride elimination from surface ethyl fragments. Similar product desorption features are observed for the reaction of ethyl iodide. However, the reaction of ethyl iodide also produces ethylene and ethane via a low temperature, desorption-limited reaction channel. It is postulated that I adatoms produced in the reaction of ethyl iodide thermal desorption might somehow promote a low temperature route to products that Cl adatoms do not.

Acknowledgements

I would like to thank Dr. David F. Cox, my advisor and the chairman of the committee, for his continued guidance, assistance, encouragement and support throughout my studies and research. I am very appreciative of his tremendous effort in correcting and polishing my thesis.

I am grateful to Drs. Richey M. Davis and S. Ted Oyama, my graduate committee, for their time in reviewing my thesis and instruction in my graduate courses.

A special thanks goes to my lab-partner Mary A. Minton for teaching me some skills in Asyst software and discussing the research with me. I wish her the best of luck in her research and career.

TABLE OF CONTENTS

LIST OF FIGURES

LIST OF TABLES

Chapter 1

Introduction

1.1 Background

Olefins are used as important chemical intermediates for a large number of industrial processes. The light alkenes such as ethylene, propylene, and butene are usually produced by the steam pyrolysis process [1,2]. The two major limitations of steam pyrolysis are the high gas temperatures (800–900 °C) required for favorable equilibrium in this endothermic process and the deposition of coke on the walls of the reactor tube that eventually require the periodic shut-down of the process for decoking [2]. To decrease the reaction temperature, there has been much recent interest in trying to find catalytic alternatives to the current industrial steam cracking process.

The catalytic dehydrogenation of alkanes has a considerable industrial impact, because it represents a route to obtain alkenes from feedstocks of low-cost saturated hydrocarbons [3,4]. In the 1970–1980s, the main interest was devoted to the catalytic dehydrogenation of *n*-butane to butene and butadiene which are precursor molecules for manufacturing synthetic rubber [5]. Nowadays, however, the dehydrogenation of propane and isobutane has become more important. Ethane dehydrogenation is an endothermic process, and requires relatively high temperatures and low pressures to obtain significant yields of ethylene [6]. Because all equivalent C–H bonds in an alkane molecule have an equal chance of reacting, a dehydrogenation reaction is expected to be rather unselective [3].

Many researchers have investigated the catalytic dehydrogenation of light alkanes as a route to obtaining alkenes for polymerization and other organic synthesis. Much of this research has focused on surveying a wide variety of both metals and metal oxides for high selectivity and conversion [5,7].

The catalytic properties of Cr_2O_3 have long been recognized [8,9]. The polymerization of ethylene over various oxides of chromium has motivated much of the research into the properties of Cr_2O_3 over the last 50 years [10]. Cr_2O_3 catalyzes many alkanes dehydrogenation reactions, such as ethane, propane, butane, pentane and hexane [3] On chromium oxide catalysts, longer hydrocarbon chains are more easily dehydrogenated than shorter ones, and straight chains are more difficult to dehydrogenate than branched ones [11]. Flick and Huff found that chromium oxide has good selectivity for ethane dehydrogenation [1], up to 60% for ethylene. Hence, chromium oxide shows promise as an effective catalyst for ethane dehydrogenation to ethylene.

The study of reactions over single crystal surfaces to model heterogeneous catalysis is a major focus of surface science [12,13,14,15,16]. By studying reactions over well-characterized surfaces, information concerning reaction site requirements, reaction pathways, and the structure sensitivity of reactions may be obtained. Although Cr_2O_3 microcrystalline powders have been extensively studied [17,18], few studies of single crystals have been reported [19,20]. In this work, by using a Cr_2O_3 $(10\bar{1}2)$ single crystal surface under ultrahigh vacuum conditions, the investigation of reaction pathways and structure-function relationships in dehydrogenation chemistry

can be made more tractable than on non-homogeneous surfaces associated with real catalysts [21].

Because of the high activation barrier for C-H bond breaking, the initial dehydrogenation step in the catalytic conversion of ethane is rate-limiting, and occurs at temperatures well above the desorption temperature for ethane from most surfaces under vacuum conditions. To circumvent this problem, ethyl fragments are produced from other reactants to bypass the initial rate-limiting dehydrogenation step. Ethyl chloride (C_2H_5Cl) and ethyl iodide (C_2H_5I) are used as ethyl fragment sources on Cr_2O_3 $(10\bar{1}2)$ surface because the C-Cl bond and C-I bond are weaker and easier to break than C-H bond.

Studies of the reactions of ethyl chloride and ethyl iodide on the Cr_2O_3 $(10\bar{1}2)$ surface are reported in chapters 2 and 3, respectively. Recommendations for future work are presented in chapter 4. Literature relevant to the topic is reviewed at the beginning of each chapter.

1.2 The Cr_2O_3 $(10\bar{1}2)$ Surface

Cr_2O_3 is an electrically insulating material (band gap=3.4 eV) with the corundum structure [22]. The coordination geometry of the bulk chromium cation is a distorted octahedron and the coordination geometry of the oxygen anion is a distorted tetrahedron. In the corundum structure, one-third of the possible cation sites are vacant along the $(10\bar{1}2)$ plane and other crystallographically equivalent planes [23].

The ideal, bulk terminated Cr_2O_3 $(10\bar{1}2)$ surface is non-polar and has the lowest energy of any perfect low-index surface of Cr_2O_3 [24]. A ball model representation of

the ideal, stoichiometric surface is shown in Figure 1.1. The $(10\bar{1}2)$ surface is somewhat corrugated or wavy due to the alternating tilt of incomplete octahedra relative to the macroscopic $(10\bar{1}2)$ plane. The topmost atomic layer of the ideal surface is composed entirely of oxygen anions. One full stoichiometric repeating unit cell normal to the surface contains five atomic layers arranged as {O, Cr, O, Cr, O}. The surface has a rectangular (almost square) periodicity with a ratio of sides a/b=0.94 [25,26]. At the $(10\bar{1}2)$ surface, all O^{2-} (oxide) anions in the top atomic layer are three coordinate and the Cr^{3+} cations in the second atomic layer are five coordinate. Both types of ions are exposed at the surface and have one degree of coordinative unsaturation relative to their bulk counterparts [23]. The surface cations are reasonably isolated with separations of ~ 3.7 Å between their nearest neighbor cations. All the ions below the top two atomic layers are fully saturated.

1.3 Experiment

The Cr_2O_3 sample used throughout this work was oriented by Laue back reflection and was mechanically polished to within ±1 degree of the $(10\bar{1}2)$ plane. The sample has an exposed surface area of approximately 77 mm^2 (about 11 mm ×7 mm) and an average thickness of 1 mm. The sample was mounted on a tantalum holder, which also acted as an indirect heating and cooling source. A type K thermocouple was attached to the rear of the sample crystal through a hole in the sample holder using AREMCO #569 ceramic cement.

All Auger electron spectroscopy (AES), low-energy electron diffraction (LEED), and thermal desorption spectroscopy (TDS) experiments were conducted in

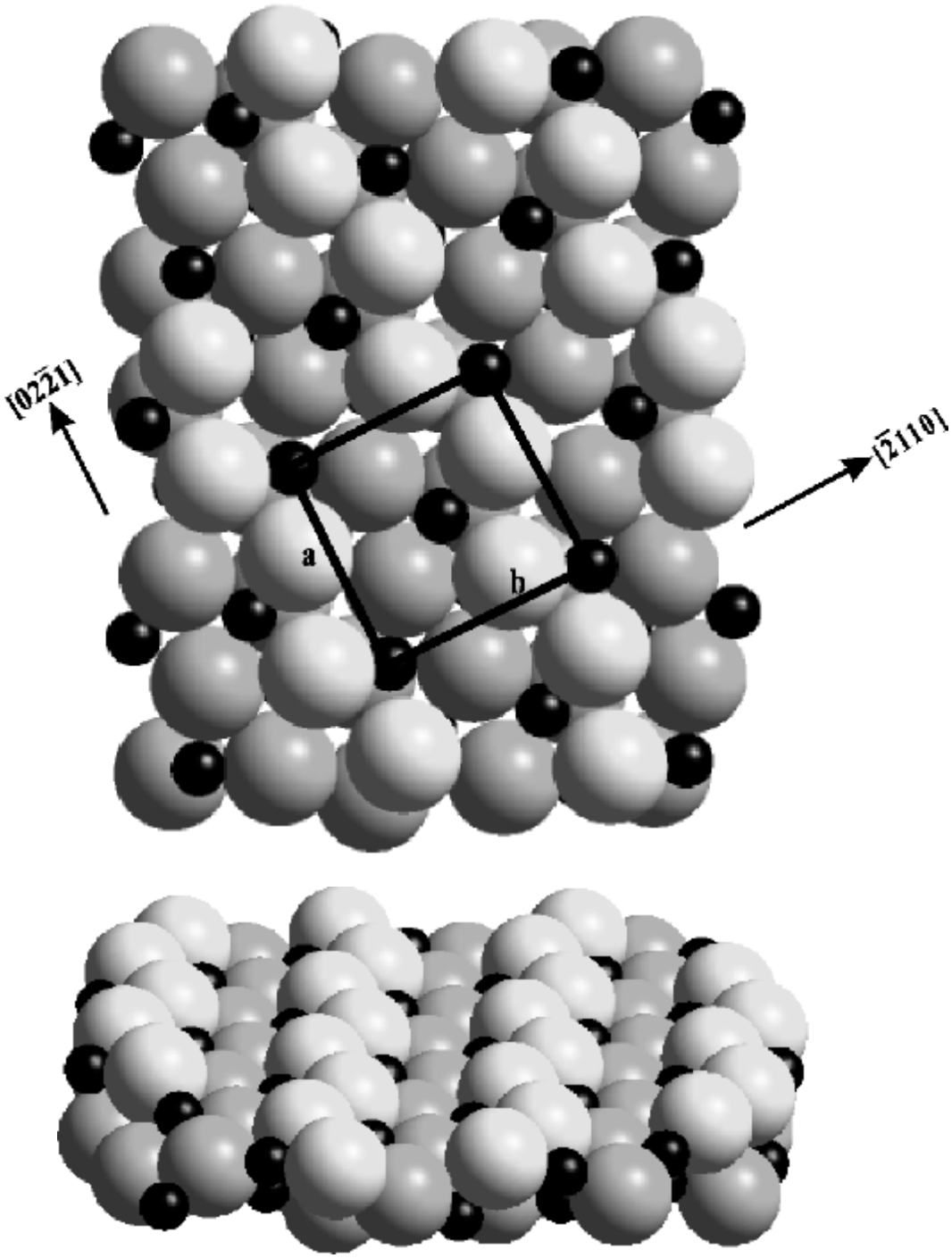

Figure 1.1 A ball model representation of the Cr_2O_3 $(10\bar{1}2)$ surface. The top view shows the $(10\bar{1}2)$ surface parallel to the plane of the page. A surface unit cell is drawn to show the periodicity. The bottom shows a side view of one stoichiometric repeating layer, which is tilted for perspective. Chromium cations are represented by the small black spheres and oxygen anions by the large gray spheres. (Reproduced with permission from Ref. 26)

an ion pumped, stainless steel ultrahigh vacuum (UHV) system having a nominal background pressure of 1×10^{-10} Torr. AES data were collected using a Perkin-Elmer model 15-155 single-pass cylindrical mirror analyzer (CMA). An incident electron beam of 5 keV was used for all Auger experiments. Spectra were collected in N(E) mode and differentiated numerically. Electron stimulated reduction of the surface did not occur during AES experiments. LEED observations were performed using Vacuum Generator 3-grid reverse view optics. A broad beam ion gun was used for sample cleaning (sputtering).

XPS measurements were performed in a separate vacuum system at the U12a beamline at the National Synchrotron Light Source. All photoemission spectra were collected at a resolution of 0.5 eV, and the spectra referenced to a Cr $2p_{3/2}$ binding energy of 576.6 eV. Compensation for surface charging during XPS was achieved with a Gammadata Scienta FG-300 flood gun using 0.5 eV electrons. The base operating pressure for this system is 1×10^{-10} Torr.

Desorbing species were monitored during TDS experiments using an Inficon Quadrex 200 quadrupole mass spectrometer. A quartz skimmer was used to minimize the desorption signal detected from the sample mounting hardware. A linear heating rate of 2.5 K/sec was used for all thermal desorption experiments to avoid thermally fracturing the ceramic sample by rapid heating. Gases were introduced into the chamber by backfilling through a variable leak valve. All doses have been corrected for ion gauge sensitivity [27].

Ion bombardment is a common method of cleaning surfaces in UHV. In this study, the sample is bombarded with 2 keV Ar^+ ions for 30 min, and then annealed to

900 K. A typical (1×1) LEED pattern obtained at a sample temperature of 775 K after such a treatment is shown in Figure 1.2.

AES measurements were conducted at 861 K to minimize the effect of sample charging. However, the overlap between this primary chromium peak and the O KLL peak in spectra makes using the Cr $L_{2,3}M_{2,3}M_{2,3}$ peak at 490 eV instead of the Cr $L_3M_{2,3}M_{4,5}$ peak at 530 eV a more reasonable choice for tracking the surface species ratio to chromium [25,26].

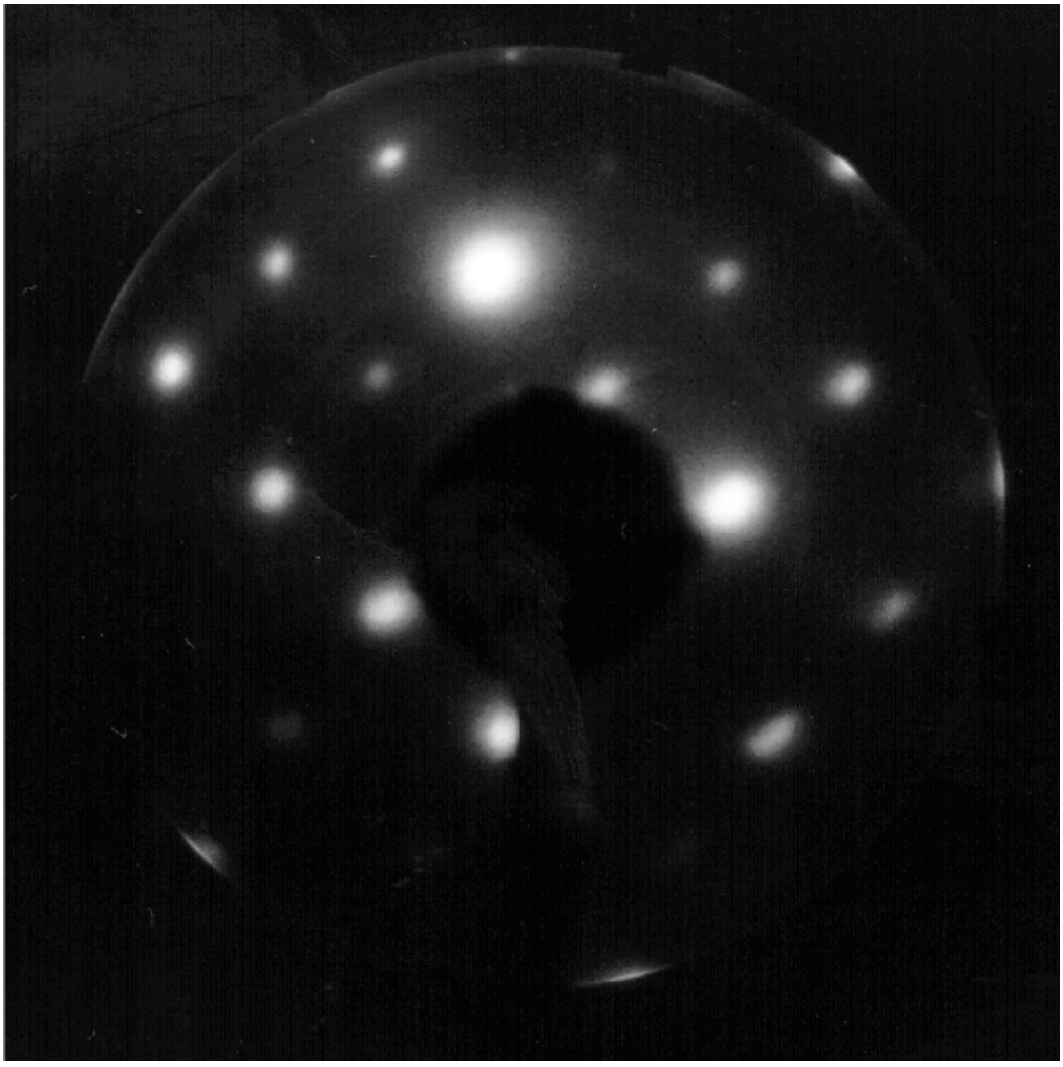

Figure 1.2 Photograph of the (1×1) LEED pattern from the Cr_2O_3 $(10\bar{1}2)$ surface taken at a sample temperature of 775 K and a beam energy of 62 eV. (Reproduced with permission from Ref. 26)

1.4 References

[1] D.W. Flick and M.C. Huff, *Applied Catalysis A: General*, **187** (1999) 13.

[2] L.F. Albright, B.L. Crynes and W.H. Corcoran, Pyrolysis: Theory and Industrial Practice, Academic Press, New York, 1983.

[3] B.M. Weckhuysen and R.A. Schoonheydt, *Catalysis Today*, **51** (1999) 223.

[4] B.M. Weckhuysen, I.E. Wachs and R.A. Schoonheydt, *Chem. Rev.* **96** (1996) 3327.

[5] S. Carra and L. Forni, *Catal. Rev.* **5** (1971) 159.

[6] J.E. Germain, Catalytic Conversion of Hydrocarbons, Academic Press, London, 1969.

[7] A. Cimino, D. Cordischi, S. Febbraro, D. Gazzoli, V. Indovina, M. Occhiuzzi and M. Valigi, *J. Mol. Catal.* **55** (1989) 2.

[8] F. Wholer and F. Mahala, *Analytical. Chemistry*, **81** (1852) 255.

[9] S.W. Weller and S.E. Voltz, *Journal of the American Chemical Society*, **76** (1954) 4695.

[10] J.L.G. Fierro and J.F.G. La Banda, *Catalysis Reviews*, **28** (1986) 265.

[11] F.E. Frey and W.F. Hupke, *Ind. Eng. Chem.* **25** (1993) 54.

[12] V.E. Henrich, *Progress in Surface Science*, **50** (1995) 77.

[13] D.P. Woodruff and T.A. Delchar, *Modern Techniques of Surface Science*, 2nd Edition, Cambridge: Cambridge University Press, 1994.

[14] W. Gopel, *Progress in Surface Science*, **20** (1985) 9.

[15] G. Pacchioni and P.S. Bagus, Adsorption on Ordered Surfaces of Ionic Solids and Thin Films, Springer-verlag, Berlin, 1993.

[16] W. Göpel, G. Rocker, and R. Feierabend, *Physical Review B*, **28** (1983) 3427.

[17] K. Hadjiivanova and G. Busca, *Langmuir*, **9** (1993) 1492.

[18] R. Fahim, M. Zaki, and N. Yacoub, *Journal of the Chemical Society, Faraday Transactions 1*, **78** (1982) 2721.

[19] V.E. Henrich and P.A. Cox, The Surface Science of Metal Oxides, Cambridge: Cambridge University Press, paperback edition, 1996.

[20] H.J. Freund, B. Dillmann, D. Erlich, M. HaBel, R.M. Jaeger, H. Kuhlenbeck, C.A. Ventrice Jr., F. Winkelmann, S. Wohlrab, C. Xu, Th. Bertrams, A. Brodde, and H. Neddermeyer, *Journal of Molecular Catalysis*, **82** (1993) 143.

[21] K.T. Queeney and C.M. Friend, *J. Phys. Chem. B*, **104** (2000) 409.

[22] D. Adler, *Solid State Physics,* **21** (1968) 83.

[23] R.J. Lad and V.E. Henrich, *Surf. Sci.* **193** (1988) 81.

[24] P.J. Lawrence, S.C. Parker and P.W. Tasker, *Communications of the American Ceramic Society*, **42** (1988) 389.

[25] S.C. York, PhD Dissertation, Virginia Tech, 1999.

[26] S.C. York, M.W. Abee and D.F. Cox, *Surf. Sci.* **437** (1999) 386.

[27] The ion gauge sensitivity factors were estimated using the correlation by S. George reported in R.L. Brainard and R.J. Madix, *J. Am. Chem. Soc.*, **111** (1989) 3826. The ion gauge sensitivity factor estimated for ethyl chloride is 4.9 and for ethyl iodide is 10.8.

Chapter 2

Reactions of Ethyl Chloride over the $Cr_2O_3(10\bar{1}2)$ Surface

2.1 Introduction

The carbon-chlorine bond of gas-phase ethyl chloride is about 85 kcal/mol, while the carbon-iodine bond of gas-phase ethyl iodide is about 55 kcal/mol [1]. The results of the chemistry of ethyl chloride on the metal surfaces, such as Ag (111) [2-6] and Pt (111) [7-10] have been reported. On the Ag (111) surface, H_2, C_2H_4, C_2H_6, 1,3-butadiene, butene and *n*-butane were observed below 400 K in thermal desorption experiments [6]. The formation of C4 products indicates that C-C bond formation reactions occur between C2 species. The lack of C3 products suggest that no C-C bond breaking occurs in the C2 fragments. All Cl accumulated on the surface desorbs as AgCl above 700 K. On Pt (111), the ethyl chloride dissociates to form surface bound ethyl fragments with coadsorbed chlorine [7]. The thermal decomposition of these ethyl groups, in the presence of Cl, occurs in at least three steps: (1) ethylene is formed just above 230 K, (2) ethylidyne ($\equiv$C-CH_3) is formed near 300 K, and (3) ethylidyne decomposes near 500 K. The thermal decomposition of the surface ethyl is accompanied by desorption of small amounts of ethane and ethylene measured by thermal desorption. Dihydrogen is desorbed as ethylidyne forms and also as it decomposes. No literature studies exist for ethyl chloride adsorption over Cr_2O_3 single-crystal surface in UHV.

2.2 Experiment

Ethyl chloride (CH_3-CH_2Cl) (Aldrich, 99.7%), ethylene (Aldrich, 99.9%) and ethane (Aldrich, 99.99%) were used as received. All reported dose sizes have been corrected by ion gauge sensitivity [11], and desorption traces have been corrected with experimentally determined mass spectrometer sensitivity factors [12].

The reaction of ethyl chloride over the nearly-stoichiometric α-$Cr_2O_3(10\bar{1}2)$ surface was investigated using thermal desorption spectroscopy (TDS) and Auger electron spectroscopy (AES). A nearly-stoichiometric surface was prepared by ion-bombardment followed by annealing the sample to 900 K. AES measurements were conducted at 861 K. Because of overlap between the primary oxygen and chromium Auger peaks, the Cr $L_{2,3}M_{2,3}M_{2,3}$ (490 eV) peak-to-peak height was used to calculate the Cl/Cr ratio. All doses for TDS experiments were performed at a sample temperature of 105 K.

2.3 Results

A combination of thermal desorption and AES results (shown below) reveals that ethyl chloride decomposes into ethyl fragments and adsorbed chlorine ($Cl_{(s)}$) on the nearly-stoichiometric α-$Cr_2O_3(10\bar{1}2)$ surface. Four products are formed from the reaction of ethyl chloride: ethylene, ethane, dihydrogen and surface chlorine adatoms. All the gas-phase products were identified by comparison of mass spectrometer cracking patterns to thermal desorption peak intensities. The relative intensities of four m/z signals were used to identify both ethylene (27, 26, 25, 24) and ethane (30, 29, 27, 26). Other products were excluded by a search that included mass numbers ranging from 2 to 200. Specifically no CO, CO_2, HI, I_2, or vinyl chloride was

observed during TDS. No surface carbon was detected with AES following the reaction of ethyl chloride.

2.3.1 Ethyl Chloride Thermal Desorption

Figure 2.1 shows representative desorption traces for the reactant and gas-phase products following the first dose in a TDS series of consecutive 0.04 L doses of ethyl chloride. One feature is apparent in the desorption spectrum of the reactant molecule (ethyl chloride) at about 417 K, while the products ethylene, ethane and dihydrogen are produced at higher temperatures. Comparisons to desorption traces for the corresponding dosed molecules indicate that the desorption kinetics of all three products are reaction limited. Ethylene production occurs at 595 K with a typical first-order desorption peak shape. Desorption of ethylene is accompanied by ethane and dihydrogen in the same temperature range. The similarity in the temperature range for desorption of ethylene, ethane and dihydrogen suggests these desorbing species originate from a common surface intermediate and share the same rate-limiting surface reaction step.

Initially, the nearly-stoichiometric $Cr_2O_3(10\bar{1}2)$ surface is reactive toward ethyl chloride, converting about 80% of the reactant to products. Figure 2.2 shows the relative amounts of gas-phase species desorbed from the surface during a series of consecutive 0.04 L doses of ethyl chloride initiated on a clean, nearly-stoichiometric surface. Desorption quantities are calculated by integrating the area under the TDS desorption curves after correcting for mass spectrometer sensitivity. The amount of ethyl chloride desorbed from the surface increases almost linearly with the consecutive doses. The amounts of all the products (ethylene, ethane and dihydrogen)

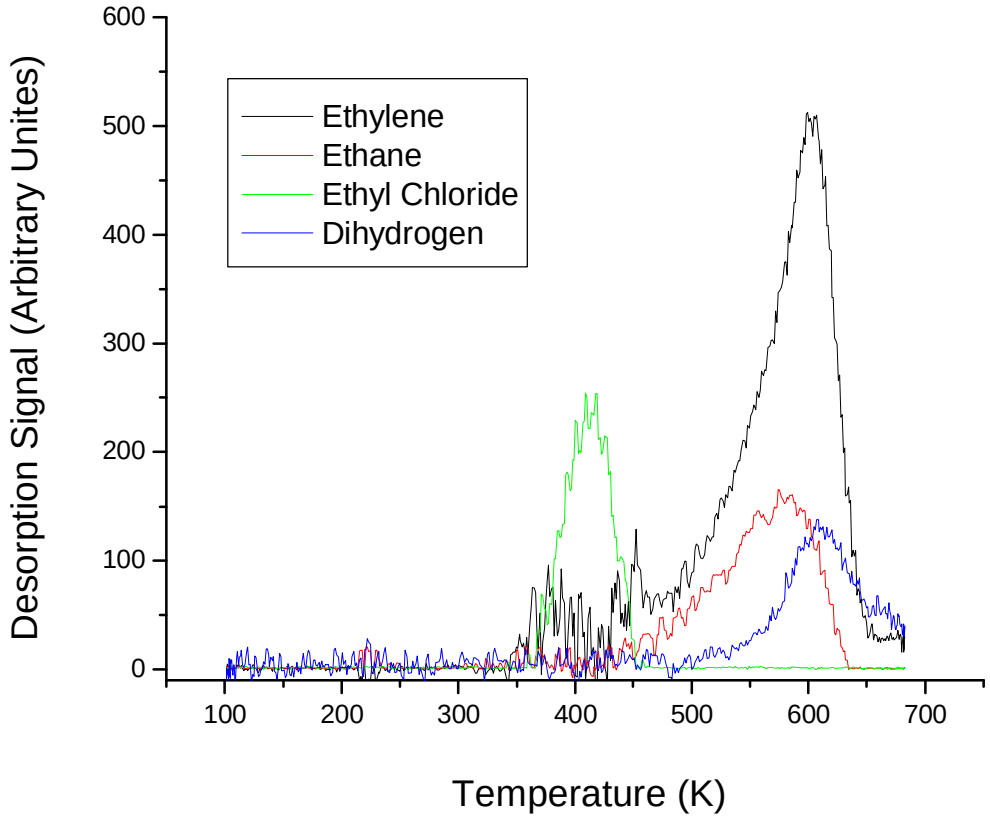

Figure 2.1 Desorption features observed following the first 0.04 L dose of CH_3-CH_2Cl in a TDS series. A desorption trace of the reactant (CH_3-CH_2Cl) is shown in green, the reaction products CH_2=CH_2 (black), CH_3-CH_3 (red) and H_2 (blue) are also shown.

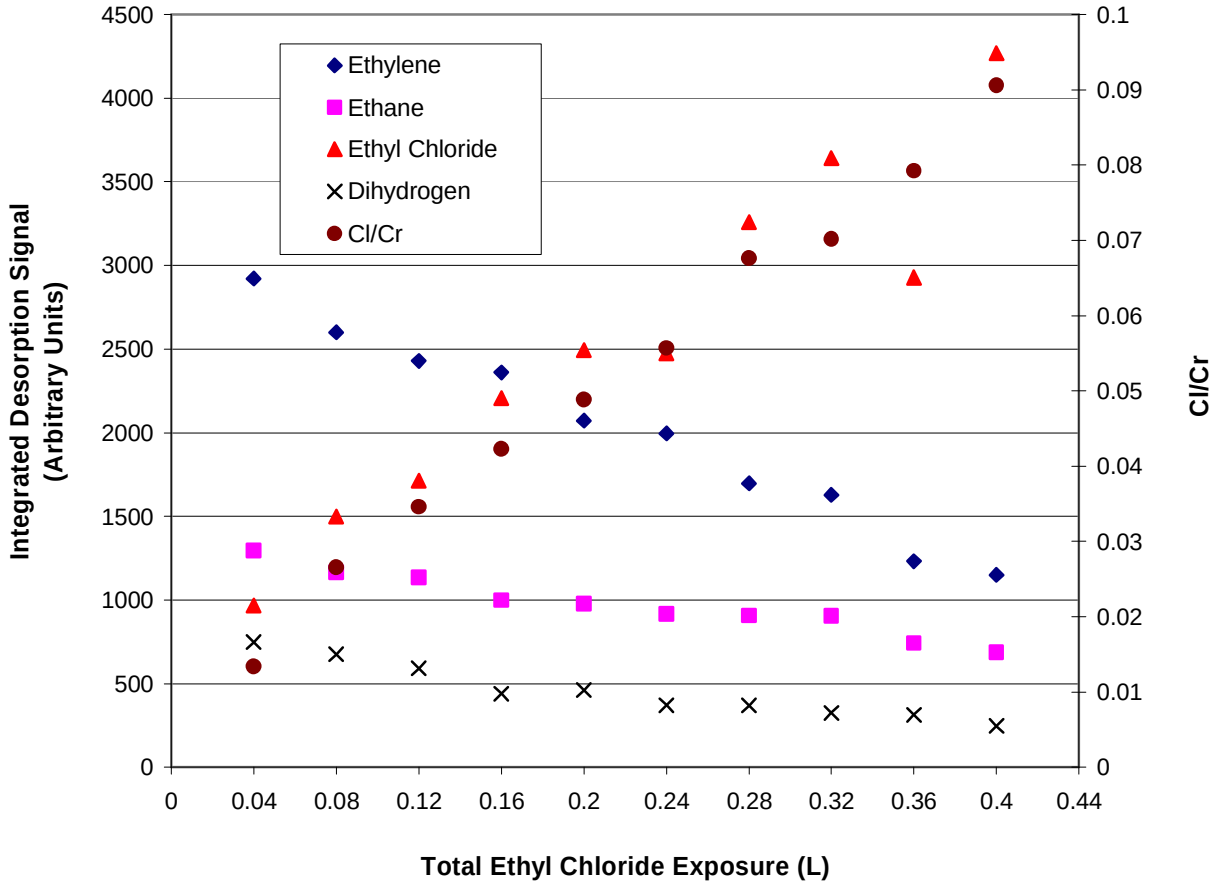

Figure 2.2 The relative desorbed quantities for each CH_3-CH_2Cl decomposition product, as well as the signal of the reactant molecule and Cl/Cr ratio, is shown above. The TDS experiment consisted of sequential 0.04 L doses over a nearly-stoichiometric Cr_2O_3 $(10\bar{1}2)$ surface.

decrease with consecutive 0.04 L doses. With each consecutive dose, Cl from ethyl chloride dissociation builds up on the surface as shown along the right hand y-axis in Figure 2.2. The decrease in the amount of products and the increase in the amount of desorbing reactant are attributable to surface deactivation associated with the build up of surface Cl with successive dose.

Figure 2.3 shows the variation in the ethylene desorption signal with consecutive 0.04 L doses starting on an initially clean, nearly-stoichiometric $(10\bar{1}2)$ surface. The $CH_2{=}CH_2$ desorption feature occurs at 595 K, and while the intensity decreases with consecutive dose, the desorption temperature remains essentially constant. Since the amount of ethylene is related to the amount of reactive surface intermediate formed, the desorption temperature is seen to be independent of the coverage of the intermediate, indicative of a first-order rate limiting step. The fixed temperature for ethylene evolution also indicates that kinetics of the reaction are unaffected by surface Cl coverage. Using the Redhead method and assuming a normal first-order pre-exponential of 10^{13} s^{-1} [13], the first-order activation energy for reaction is estimated to be about 157 kJ/mol.

In addition to the ethylene desorption signals seen in Figure 2.3, noisy features are observed in all the traces between 340 and 480 K. These features are the result of small subtraction errors where the m/z=27 signal used to follow ethylene are corrected by subtraction to remove a very large contributions due to ethyl chloride for this cracking fragment. These remaining noisy features do not represent anything of chemical significance.

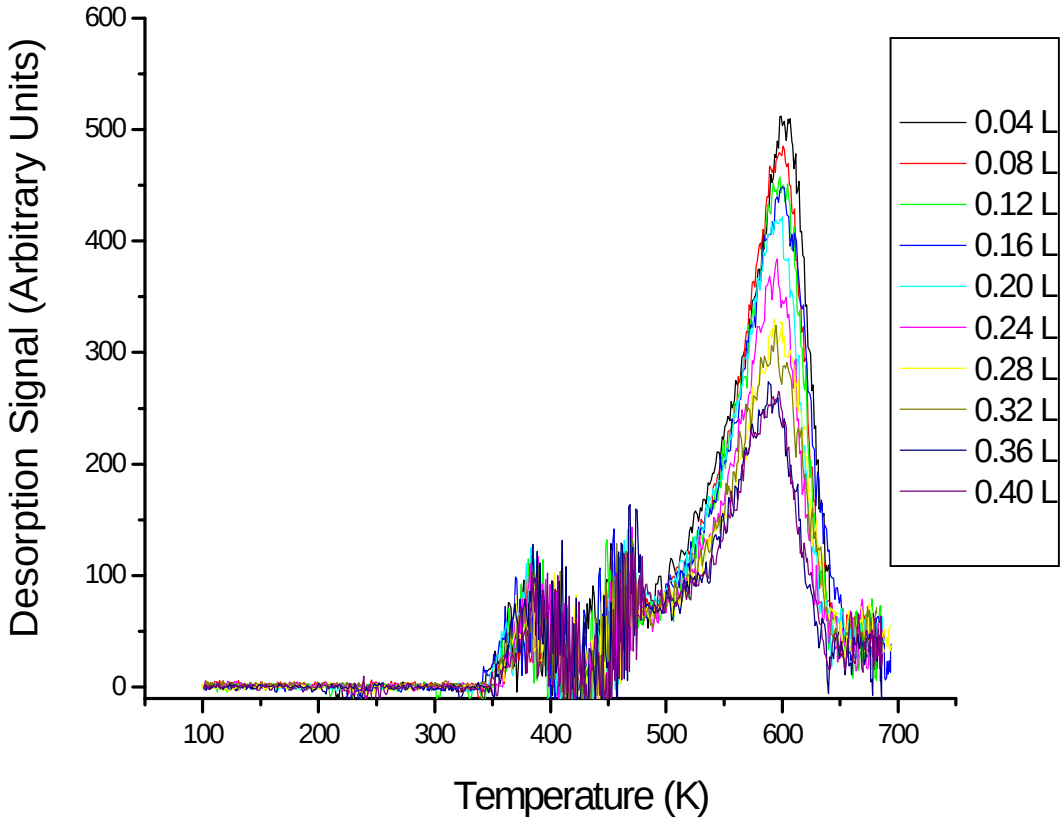

Figure 2.3 Desorption traces of the CH_2=CH_2 product for a series of consecutive 0.04 L ethyl chloride doses over a nearly-stoichiometric $Cr_2O_3(10\bar{1}2)$ surface.

Unlike the constant temperature observed above for ethylene, variations are observed (not shown) in the desorption temperature of the ethyl chloride reactant as a function of consecutive dose. As in Figure 2.1, one ethyl chloride desorption feature is observed at about 415 K for the first 0.04 L dose on a clean surface. The feature increases in intensity with consecutive dose as illustrated in Figure 2.2, and the desorption temperature increases to about 435 K following by the tenth dose. The small increase in desorption temperature suggests a small increase (~ 5 kJ/mol) in the heat of adsorption of molecular ethyl chloride due to surface modification by deposited chlorine adatoms. The nature of this stabilization is not understood.

2.3.2 Post-reaction AES

Figure 2.4 shows a typical set of AES spectra collected before and after a series of consecutive ethyl chloride TDS experiments. After a total exposure of 0.4 L of ethyl chloride by successive 0.04 L doses and TDS runs, a chlorine feature is clearly observed using AES at Kinetic Energy 190 eV (comparing the top and the bottom panels, the features between 450-600 eV are from chromium and oxygen). Chlorine adatoms are deposited as a result of the reaction of ethyl chloride**.** Since previous work has shown that Cl binds at surface Cr cations with a Cl/Cr ratio of 0.32 corresponding to a coverage equivalent to one Cl adatom for every surface Cr cation [14,15], the Cl/Cr ratio of 0.09 obtained from Figure 2.4 indicates that about 30% of the chromium cations on the Cr_2O_3 $(10\bar{1}2)$ surface are covered by chlorine atoms following the TDS experiments.

The AES data demonstrates that as the amount of products detected in the TDS runs declines, the surface Cl/Cr ratio increases (see Figure 2.2). The relation suggests

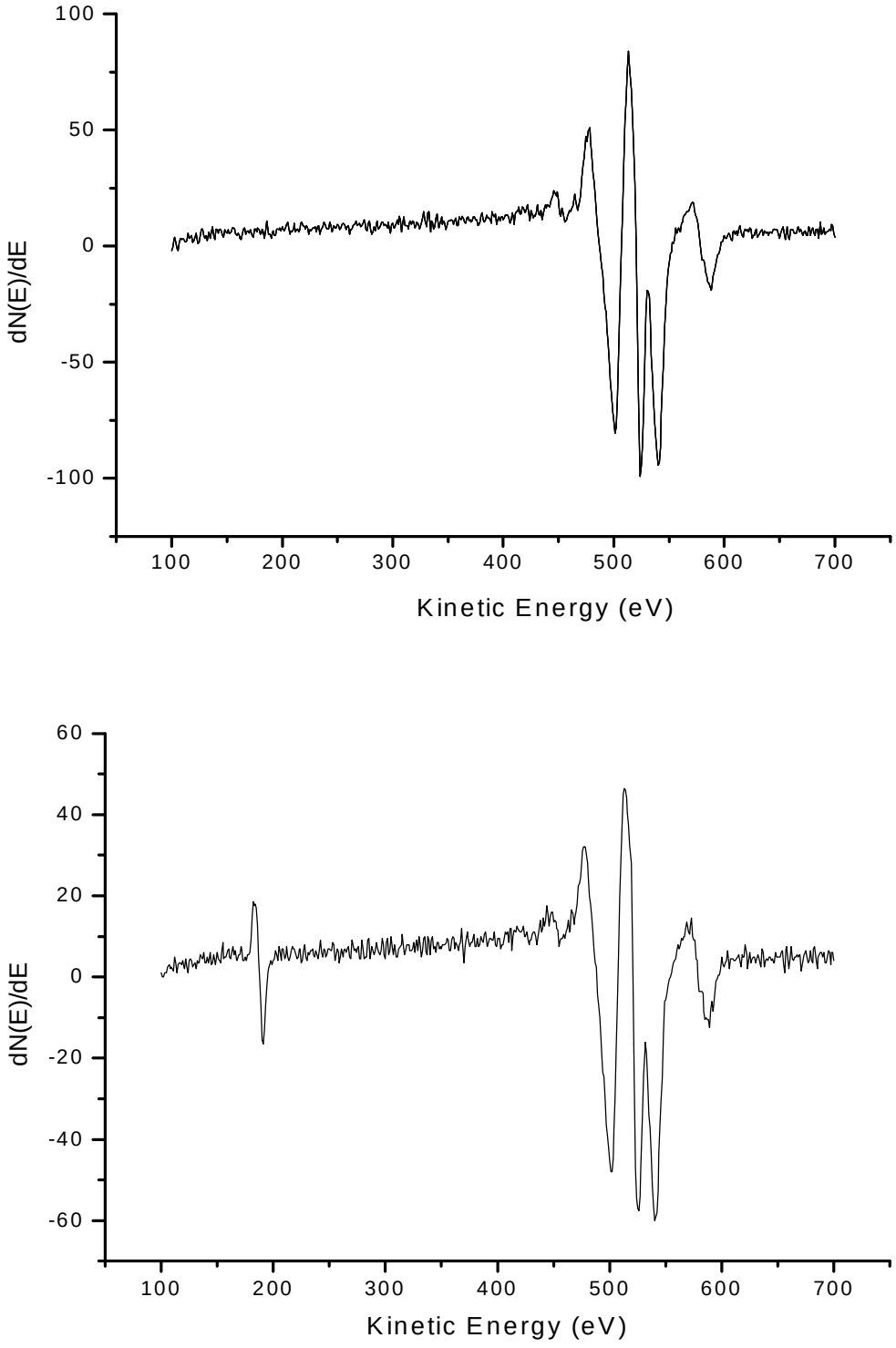

Figure 2.4 An AES spectrum of a (1×1) nearly-stoichiometric $Cr_2O_3(10\bar{1}2)$ surface. Top: the clean surface before TDS. Bottom: the surface after total 0.4 L ethyl chloride exposure (dose at 105 K).

the deposition of chlorine onto the sample surface is coincident with changes in surface reactivity and the loss activity of the surface towards products. The surface chlorine adatoms cause surface deactivation by site-blocking of the active Cr^{3+} surface cations. It should be noted that no surface carbon is produced, indicating that surface fragments do not undergo C-C bond cleavage and complete dehydrogenation coke. No evidence is seen for the replacement of lattice oxygen by chlorine on the nearly-stoichiometric Cr_2O_3 $(10\bar{1}2)$ surface, because no oxygen contained compound is observed.

2.4 Discussion

The weakest bond in CH_3-CH_2Cl is C-Cl with a bond energy of 85 kcal/mol [1]. From the AES results, it is clear that chlorine adatoms are deposited on the nearly-stoichiometric Cr_2O_3 $(10\bar{1}2)$ surface during thermal desorption experiments. It is reasonable, therefore, to assume that the initial reaction step is the dissociation of adsorbed CH_3-CH_2Cl via carbon-chlorine bond cleavage as seen previously on Ag [6,7]. Dissociation of CH_3-CH_2Cl then gives surface ethyl fragments and adsorbed chlorine atoms. The reaction limited chemistry producing ethylene, ethane and dihydrogen near 595 K is readily explained in terms of the decomposition of an ethyl fragment reaction intermediate. Rate limiting β-hydride elimination directly forms ethylene, CH_2=CH_2. The liberated hydrogen atoms are then free to react with remaining surface ethyl fragments to form ethane, or may react with other surface hydrogen atoms to form dihydrogen. The proposed reaction mechanism may be represented by the following sequence of elementary steps:

$CH_3\text{-}CH_2Cl \rightarrow CH_3\text{-}CH_{2\,(S)} + Cl_{(S)}$

$CH_3\text{-}CH_{2\,(S)} \rightarrow CH_2{=}CH_{2\,(g)} + H_{(S)}$ (rate-limiting step)

$CH_3\text{-}CH_{2\,(S)} + H_{(S)} \rightarrow CH_3\text{-}CH_{3\,(g)}$

$H_{(S)} + H_{(S)} \rightarrow H_{2\,(g)}$

In the catalysis literature, deactivation of powdered Cr_2O_3 catalysts has been attributed to carbon deposition [16], and to the formation of inactive crystalline phases at the surface that isolate cations from the surface [17]. In this work, no carbon residue is deposited on the $Cr_2O_3(10\bar{1}2)$ surface as a result of ethyl fragment decomposition and dehydrogenation under the conditions of our experiments. These results suggest that ethyl fragments may not be a primary intermediate in coking chromia surfaces during ethane dehydrogenation.

2.5 Conclusions

The reaction of ethyl chloride over a nearly-stoichiometric $Cr_2O_3(10\bar{1}2)$ surface has been investigated under UHV conditions. The products are ethylene, ethane, dihydrogen and adsorbed chlorine. For all the gas phase products, first-order β-hydride elimination from surface ethyl fragments is the rate-limiting reaction step with an activation energy of 157 kJ/mol.

The deposition of chlorine on the surface decreases surface activity and lead to deactivation of the surface due to sites blocking of Cr^{3+} cations. No evidence is seen for the replacement of surface lattice oxygen by chlorine because no oxygen contained desorption species detected, and no carbon is detected on the deactivated surface.

2.6 References

[1] J.L. Lin and B.E. Bent, *J. Phys. Chem.* **96** (1992) 8529.

[2] X.L. Zhou and J.M. White, *Surface Science*, 241 (1991) 244.

[3] Z.M. Liu, Z.L. Zhou and J.M. White, *Chem. Phys. Lett.* **1998** (1992) 615.

[4] X.L. Zhou and J.M. White, *Chem. Phys. Lett.* **167** (1990) 205.

[5] J.M. White, *Langmuir,* **10 (**1994) 3946.

[6] X.L. Zhou, P.M. Blass, B.E. Koel and J.M. White, *Surface Science*, 271 (1992) 452.

[7] K.G. Lloyd, B. Roop, A. Campion and J.M. White, *Surface Science*, **214** (1989) 227.

[8] S.K. Jo, J. Kiss, J.A. Polanco and J.M. White, *Surface Science*, **253** (1991) 233.

[9] N. Freyer, G. Pirug and H.P. Bonzel, *Surface Science* **126** (1983) 487.

[10] K.G. Lloyd, A. Campion and J.M. White, *Catal. Lett.* **2** (1989) 105.

[11] The ion gauge sensitivity factor for ethyl chloride was estimated as 4.9 using the correlation by S. George reported in R.L. Brainard and R.J. Madix, *J. Am. Chem. Soc.*, **111** (1989) 3826.

[12] Mass spectrometer sensitivity factors for ethyl chloride (m/z 64), ethylene (m/z 27), ethane (m/z 30), and dihydrogen (m/z 2) were 0.15, 0.68, 0.27 and 1.04, respectively.

[13] P.A. Redhead, *Vacuum,* **12** (1962) 203.

[14] S.C. York, PhD Dissertation, Virginia Tech, 1999.

[15] S.C. York and D.F. Cox, *J. Phys. Chem. B*, **107** (2003) 5182.

[16] L.E. Manzer and V.N.M. Rao, *Advances in Catalysis,* **39** (1993) 329.

[17] E. Kemnitz, A. Kohne, I. Grohmann, A. Lippitz, and W.E.S. Unger, *Journal of Catalysis,* **159** (1996) 270.

Chapter 3

Reactions of ethyl iodide over the $Cr_2O_3(10\bar{1}2)$ Surface

3.1 Introduction

Ethyl iodide (C_2H_5I) is commonly used as a source of ethyl fragments on metal surfaces because the C-I bonds are weaker and easier to break than C-H bonds [1]. Ethyl iodide has been studied on Al (100) and Al (111) surfaces by Bent et al. [2], on a Pd (100) surface by Kovacs and Solymosi [3], and on a Ni (100) surface by Tjandra and Zaera [4]. The only gas-phase products from these surfaces are ethylene, ethane and dihydrogen. On the Pd (100) surface, surface carbon is formed after heating over 450 K. No surface C has been reported on Al (100), Al (111) and Ni (100) surfaces Karamullaoglu et al. [5] and Michalakos et al. [6] have reported that the dominant pathway for activating surface ethyl fragments is through β-hydride elimination to form ethylene and the elimination of α-hydride which would result in degradation products, such as coke. On the Pt (111) surface, the products from ethyl iodide are methane, ethane and ethylene. The forming of methane indicates some carbon-carbon bonds are broken [7]. On Au (100) and Au (111) surfaces, ethylene, ethane and butane are observed, indicating carbon-carbon bonds are formed by ethyl fragment coupling [8,9]. On an Ag (111) surface, butane is the only product from dosed ethyl iodide [10], no C-C or C-H bond cleavage occurs. No literature studies exist for ethyl iodide adsorption over Cr_2O_3 single-crystal surfaces in UHV.

3.2 Experiment

Ethyl iodide (CH_3-CH_2I) (Aldrich, 99%) was purified by freeze-pump-thaw cycles and flash distillation. Ethylene (Aldrich, 99.9%) and ethane (Aldrich, 99.99%) were used as received. All reported dose sizes have been corrected by ion gauge sensitivity [11], and desorption traces have been corrected with experimentally determined mass spectrometer sensitivity factors [12].

The reaction of ethyl iodide over the nearly stoichiometric α-$Cr_2O_3(10\bar{1}2)$ surface was investigated using thermal desorption spectroscopy (TDS), Auger electron spectroscopy (AES), and X-ray photoelectron spectroscopy (XPS). A nearly stoichiometric surface was prepared by ion-bombardment followed by annealing the sample to 900 K. AES measurements were made at 861 K to minimize sample charging. The iodine Auger peak falls in the same kinetic energy range of oxygen and chromium, so AES is not useful for quantifying the amount of surface iodine. For TDS experiments, all doses were made at a sample temperature of 105 K.

3.3 Results

A combination of thermal desorption and XPS results (shown below) reveals that ethyl iodide decomposes into ethyl fragments and adsorbed iodine ($I_{(s)}$) on the stoichiometric α-$Cr_2O_3(10\bar{1}2)$ surface. Four products are made from the reaction of ethyl iodide: ethylene, ethane, dihydrogen and surface iodine adatoms. All the gas-phase products are identified by comparison of mass spectrometer cracking patterns to thermal desorption peak intensities. The relative intensities of four m/z signals are used to identify both ethylene (27, 26, 25, 24) and ethane (30, 29, 27, 26). Other products are excluded by a search that included mass numbers ranging from 2 to 200.

Specifically no CO, CO_2, HI, I_2, or vinyl iodide was observed during TDS. No surface carbon is detected with AES following the reaction of ethyl iodide.

3.3.1 Ethyl Iodide Thermal Desorption

Figure 3.1 shows representative desorption traces for the gas-phase products following the first dose in a series of consecutive 0.04 L doses of ethyl iodide. Nearly 100% of the ethyl iodide is converted to products during initial TDS runs. The ethyl iodide trace shown in the figure is from the fifth 0.04 L dose (enlarged by a factor of five), and shows reactant ethyl iodide desorption at about 480 K. The gas-phase products are ethylene, ethane and dihydrogen. The products evolve together in a reaction-limited, high temperature feature with an ethylene desorption temperature of 580 K, similar to the product features seen for the reaction of ethyl chloride in Chapter 2. This high temperature reaction is attributed to a rate limiting β-hydride elimination from a surface ethyl fragment, as described in Chapter 2. Additionally, lower temperature desorption features are observed for ethane and ethylene at about 210 K and 340 K, respectively.

Figure 3.2 shows the relative amounts of gas-phase species desorbed from the surface during a series of consecutive 0.04 L doses of ethyl iodide initiated on a clean, nearly-stoichiometric surface. Desorption quantities are calculated by integrating the area under the TDS desorption curves and correcting for mass spectrometer sensitivity. Initially, the nearly-stoichiometric $Cr_2O_3(10\bar{1}2)$ surface is very reactive toward ethyl iodide, converting nearly 100% of the reactant to products. The amount of ethyl iodide desorbed from the surface is negligible following the first four doses, but increases in amount with subsequent doses. Ethyl iodide desorption occurs at

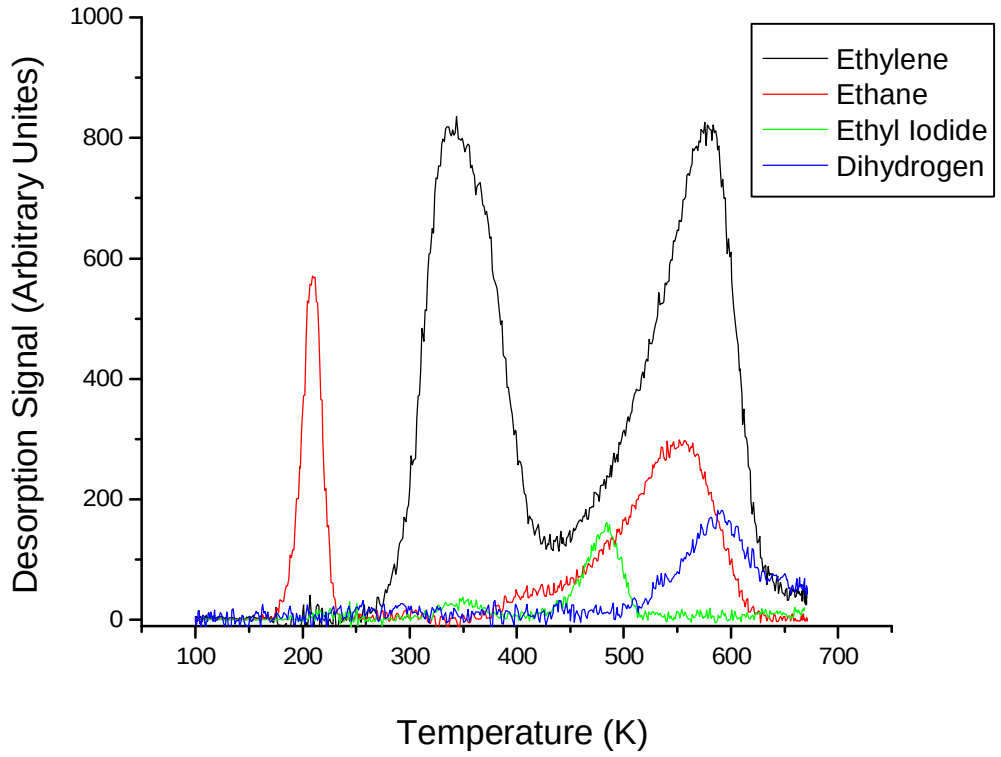

Figure 3.1 Desorption features observed following the first 0.04 L dose of CH_3-CH_2I on a clean, nearly-stoichiometric surface. A desorption trace of the reactant (CH_3-CH_2I) is shown in green (this trace is from the 5th 0.04 L dose and enlarged 5 times), the reaction products CH_2=CH_2 (black), CH_3-CH_3 (red) and H_2 (blue) are also shown.

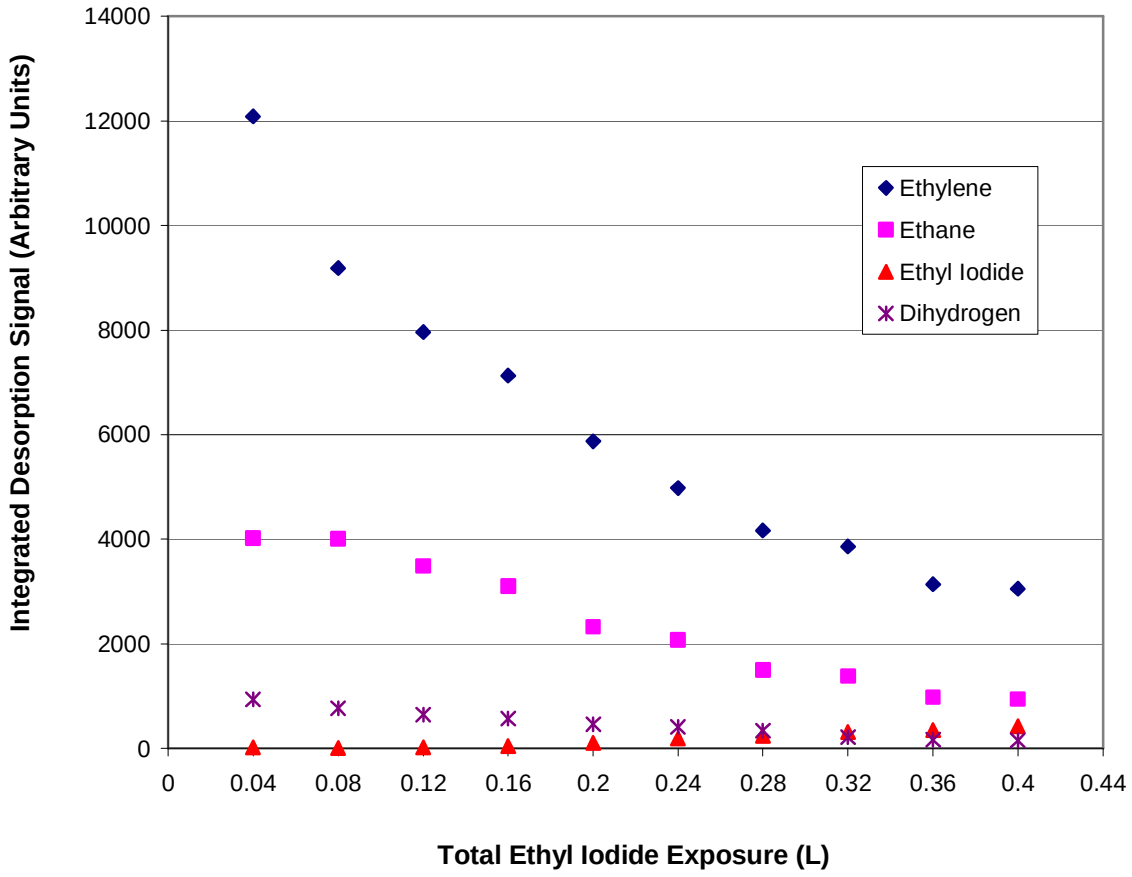

Figure 3.2 The relative quantities desorbed for each CH_3-CH_2I decomposition products, as well as the signal of the reactant molecule are shown above. The TDS experiment consisted of sequential 0.04 L doses over a nearly-stoichiometric Cr_2O_3 $(10\bar{1}2)$ surface.

about 480 K (Figure 3.1), and the desorption temperature remains constant with subsequent doses as the amount desorbed increases.

Figure 3.2 also shows that the amounts of gas phase products (ethylene, ethane and dihydrogen) tend to decrease with successive dose. The decrease in products occurs as the amount of reactant (ethyl iodide) desorption increases. The decrease in products and increase in reactant shows that the surface becomes deactivated with successive dose. The reason for the deactivation is similar to that observed with ethyl chloride. Surface cations become halogenated (in this case with iodine adatoms from ethyl iodide dissociation), which blocks the reactive surface cations (see XPS data below).

The primary difference in the thermal desorption results for ethyl chloride in Chapter 2 and those for ethyl iodide is the appearance of the low temperature features for products ethane (near 210 K) and ethylene (near 340 K). These low temperature reaction channels are not observed with the ethyl chloride reactant. Figure 3.3 shows the separate variation in amounts of low and high temperature product features for ethylene and ethane as a function of consecutive 0.04 L dose. The amount of ethylene observed in the low temperature feature decreases much more rapidly than that observed in the high temperature feature. For ethane, the amount observed in the low temperature feature tends to be only about 1/3 or less of that seen in the high temperature feature.

To understand the kinetics of the low temperature product desorption signals, the ethane and ethylene product signals from ethyl iodide have been compared to desorption traces for dosed ethane and ethylene. Figure 3.4 shows the comparison for

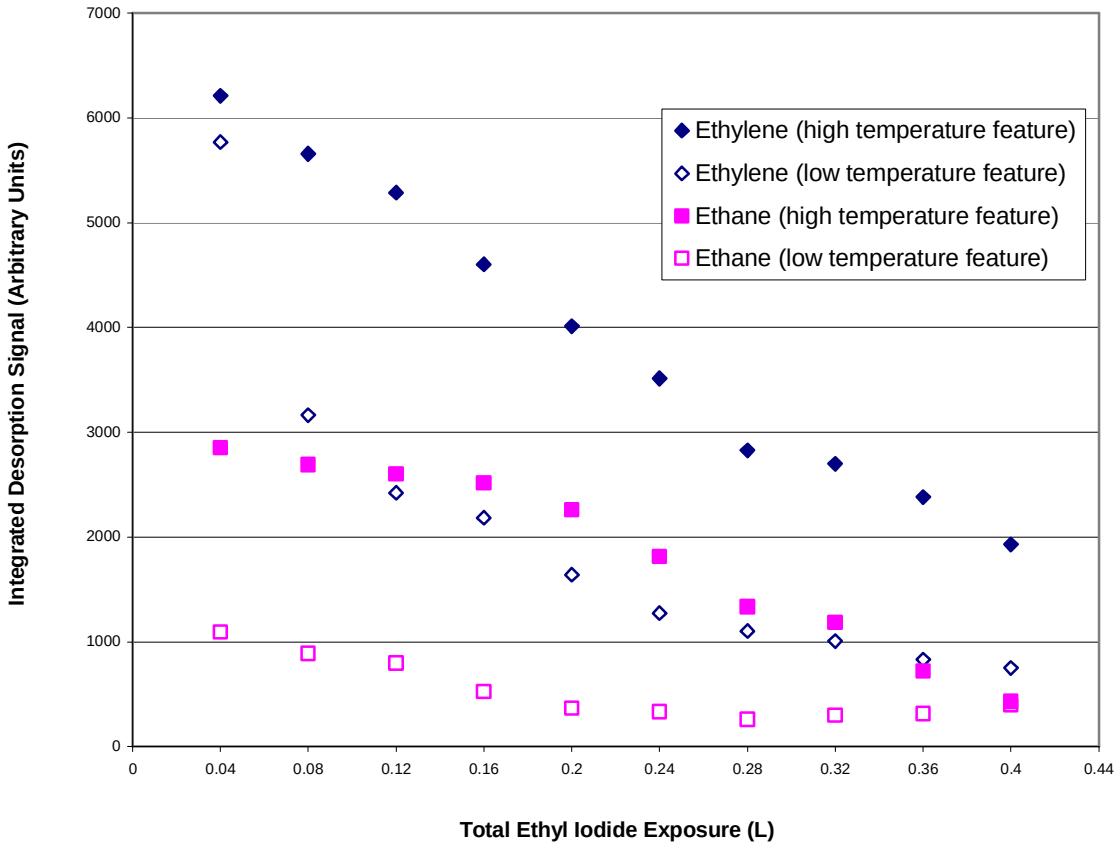

Figure 3.3 The relative ethylene and ethane quantities desorbed for CH_3-CH_2I decomposition are shown above. The TDS experiment consisted of sequential 0.04 L doses over a nearly-stoichiometric Cr_2O_3 $(10\bar{1}2)$ surface.

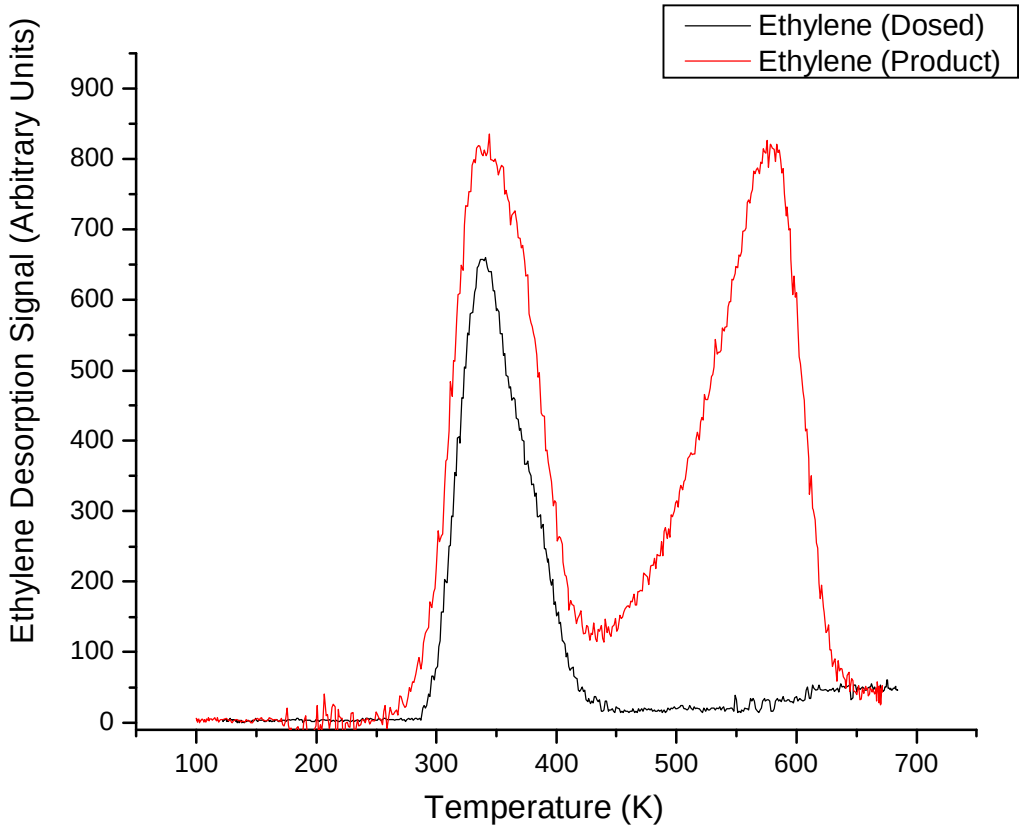

Figure 3.4 Comparison of TDS trace of CH_2=CH_2 product from 0.04 L ethyl iodide decomposition with the trace obtained from dosed ethylene (0.025 L) on a nearly-stoichiometric $Cr_2O_3(10\bar{1}2)$ surface. The high temperature feature is absent from the dosed ethylene trace.

ethylene. The trace for dosed ethylene matches the low temperature ethylene product feature from ethyl iodide, indicating that the low temperature feature is associated with the desorption of molecularly adsorbed (chemisorbed) ethylene; i.e., the low temperature channel is desorption limited. As described in Chapter 2, the high temperature reaction channel to ethylene is reaction limited. Figure 3.5 shows the comparison for ethane. The trace for dosed ethane matches the low temperature product feature from ethyl iodide, indicating that the low temperature feature is desorption limited, and associated with the desorption of molecularly adsorbed ethane. Again, as described in Chapter 2, the high temperature reaction channel to ethane is reaction limited.

As reported by Lin and Bent [13], the carbon-iodine bond of gas-phase ethyl iodide is about 55 kcal/mol, while the carbon-chlorine bond of gas-phase ethyl chloride is about 85 kcal/mol. Hence, ethyl iodide is much easier to dissociate than ethyl chloride. Comparison of the product yields for the similar doses (0.04 L) ethyl chloride and ethyl iodide shows that ethyl chloride produces only 24% of the ethylene and 32% of the ethane produced by ethyl iodide. The difference in C-X bond energies appears to be primarily responsible for these large differences in reactivity.

3.3.2 XPS Results

Figure 3.6 shows I $3d_{5/2}$ and C 1s spectra following a 100 L exposure of ethyl iodide adsorbed on the clean, nearly-stoichiometric $Cr_2O_3(10\bar{1}2)$ surface at 120 K. The sample was heated to sequentially higher temperatures, then cooled back to 120 K to take the XPS spectra. Table 3.1 contains XPS data for the binding energy (BE) and full width at half maximum (FWHM).

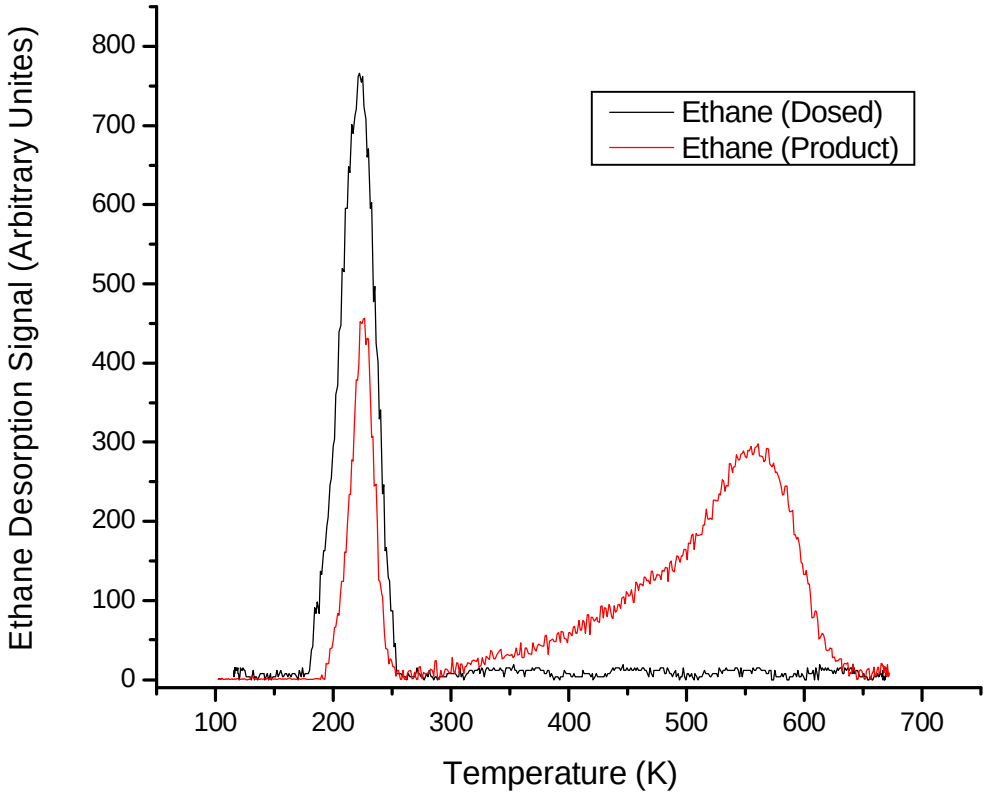

Figure 3.5 Comparison of TDS trace of CH_3-CH_3 product from the 2nd dose 0.04 L ethyl iodide decomposition with the trace obtained from dosed ethane (0.02 L) on a nearly-stoichiometric $Cr_2O_3(10\bar{1}2)$ surface. The high temperature feature is absent from the dosed ethane trace.

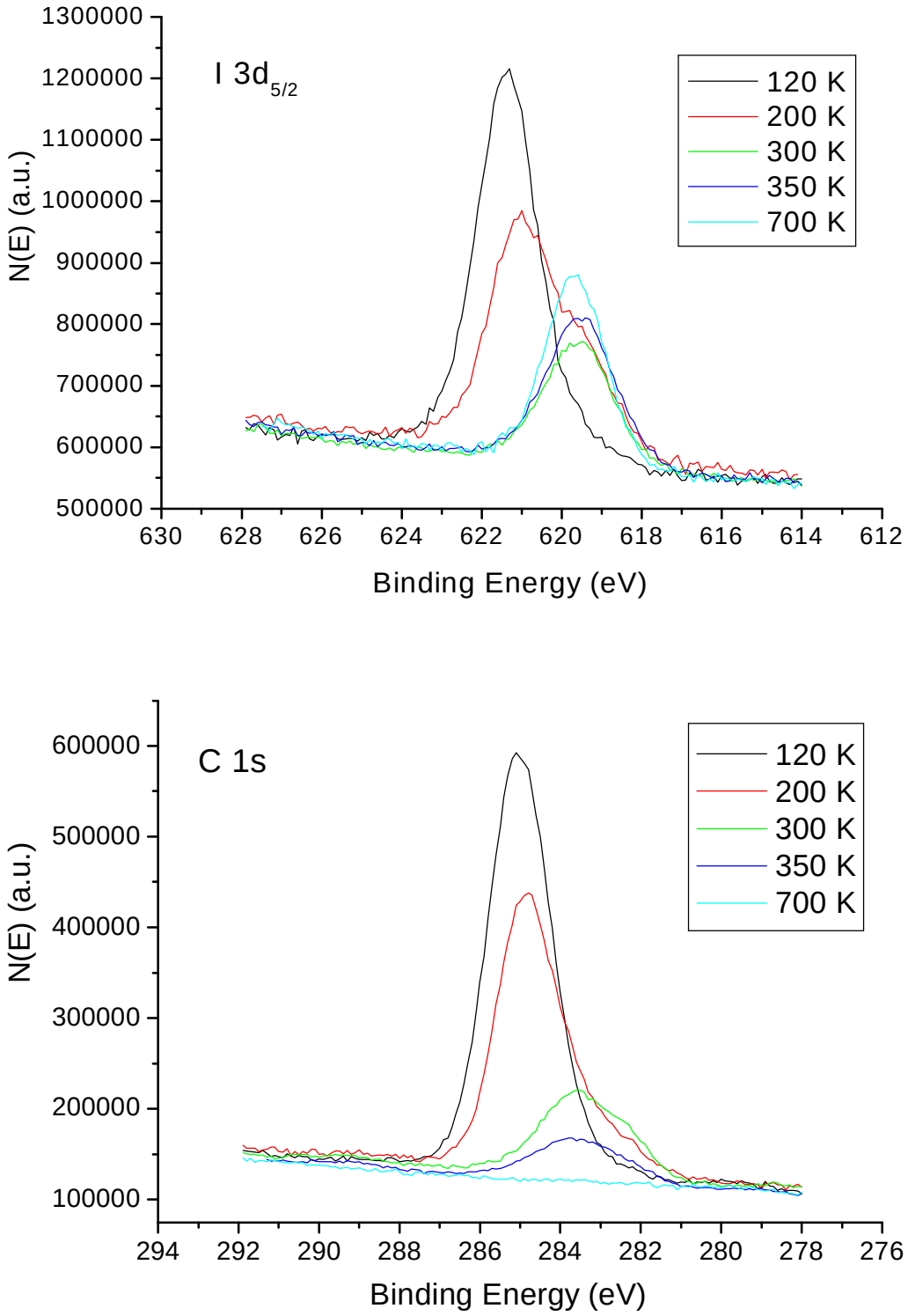

Figure 3.6 XPS data for a 100.0 L CH_3-CH_2I dose on a nearly-stoichiometric surface at 120 K. The top panel shows I $3d_{5/2}$ spectra (photon energy: 700 eV) and the bottom shows C 1s spectra (photon energy: 350 eV).

T (K)	C 1s BE (eV)	C 1s FWHM (eV)	I $3d_{5/2}$ BE (eV)	I $3d_{5/2}$ FWHM (eV)
120	285.1	1.8	621.3	1.8
200		2.0		2.6
300		2.8	619.5	2.0
350	283.7	2.6	619.5	1.9
700	------	----	619.6	1.8

Table 3.1 XPS data for a 100 L CH_3CH_2I dosed on the nearly-stoichiometric Cr_2O_3 $(10\bar{1}2)$ surface.

In the top panel of Figure 3.6, the binding energy observed for I $3d_{5/2}$ is 621.3 eV with a FWHM of 1.8 eV for a large coverage of molecular (multilayer) CH_3CH_2I at 120 K. This binding energy is assigned to I $3d_{5/2}$ of molecular ethyl iodide. The I $3d_{5/2}$ feature broadens (FWHM=2.6 eV compared to 1.8 eV) following heating to 200 K, suggesting the possibility of at least two iodine species. Heating to 300 K narrows the feature and gives a binding energy of 619.5 eV. Heating to 350 K and 700 K gives similar features. The decrease in binding energy is consistent with dissociation via C-I bond breaking to give surface iodine adatoms [3,4,7]. The I $3d_{5/2}$ results indicate that by a temperature of 300 K the majority of adsorbed molecular ethyl iodide either dissociates or is desorbed. The results also indicate that iodine adatoms remain on the surface after heating to temperatures well above those where gas phase products are evolved in thermal desorption.

In the bottom panel of Figure 3.6, the C 1s binding energy observed is 285.1 eV (see Table 3.1) with a FWHM of 1.8 eV for a large coverage of molecular (multilayer) CH_3CH_2I at 120 K. The single feature suggests that the binding energy for the carbon atoms in the ethyl group and the iodine containing end of molecular ethyl iodide cannot be resolved. After heating to 200 K, the C 1s signal broadens to lower binding energies (FWHM 2.0 eV), suggesting at least two separate contributions to the feature. Possibilities suggested by the thermal desorption results include C 1s contributions from molecular ethyl iodide, ethyl fragments, and adsorbed ethane and ethylene. After heating to 300 K, the C 1s feature clearly shifts to lower binding energies, with the FWHM increasing to 2.8 eV. Contributions to the C 1s feature following this annealing treatment likely include both ethyl fragments and ethylene. Following

heating to 350 K, the C 1s feature appears more symmetric with a FWHM of 2.6 eV. Since thermal desorption results indicate that the only remaining surface species are those associated with the high temperature reaction channel, this spectrum is likely characteristic of surface ethyl fragments. Note that the XPS binding energy indicates the ethyl fragments are bound to surface Cr centers, since significantly higher binding energies (286.0 eV or greater) would be expected for an alkoxide (O-bound) fragment [14]. Heating to 700 K removes all the carbon contained species from the surface.

3.4 Discussion

The high temperature reaction channel observed in thermal desorption experiments with ethyl iodide is similar to that observed for ethyl chloride. The similarity indicates that the origin of this reaction channel is the same for both reactant molecules. As described in Chapter 2, the high temperature chemistry is readily explained in terms of a rate limiting step involving β-hydride elimination from a surface ethyl fragment. There is a minor difference of about 15 K in the ethyl fragment decomposition temperature (i.e., the ethylene desorption temperature) for the two molecules, corresponding to an approximate difference of 4 kJ/mol in the activation energy. The higher values for ethyl chloride may be associated with a minor stabilizing effect of surface Cl adatoms on the ethyl fragment reaction intermediate. Such an effect of surface Cl has been observed for the decomposition of surface vinyl groups in separate experiments [15].

The primary difference between the reactions of ethyl chloride and ethyl iodide are the low temperature, desorption limited ethylene and ethane produced from ethyl iodide. The origin of these low temperature products is not well understood. However,

since both ethane and ethylene are desorption limited, the reaction(s) that generate these products must occur at or below the ethane desorption temperature. The only difference between the two reactants is the identity of the halogen atom deposited on the surface as a result of C-halogen bond breaking. One explanation for the origin of the desorption limited products might be that iodine adatoms somehow promote a low temperature route to products that Cl adatoms do not. Since the products are identical to those observed at higher temperatures, it is possible that any such low temperature pathway still involves dehalogenation and H elimination, but with a significantly lower activation barrier to reaction. No dihydrogen desorption occurs at low temperature, suggesting that any released H atoms are readily scavenged by the remaining ethyl fragment to form ethane. In support of this idea, preliminary experiments have been done. The surface was first predosed and reacted with ethyl iodide to deposit I adatoms prior to adsorbing and reacting ethyl chloride. The results give a small desorption signal of ethane at low temperature from ethyl chloride. However, the results are inconclusive because sometimes the thermal desorption for ethyl chloride in the absence of iodine gives a small low temperature ethane desorption signal. Further experiments are needed.

An alternate explanation might involve the differences in the C-X (X=halogen atom) bond strength for the two reactants. The gas phase C-I bond strength in ethyl iodide is about 55 kcal/mol, 30 kcal/mol lower than the C-Cl bond in ethyl chloride [13]. It is possible that ethyl iodide undergoes a partial reaction to ethane and ethylene in the gas manifold lines as a result of the lower C-X bond strength, and is subsequently dosed onto the sample along with the ethyl iodide. This explanation

seems less likely since care was taken in reactant purification and pretreatment (conditioning) of the manifold.

3.5 Conclusions

The reaction of ethyl iodide over a nearly stoichiometric $Cr_2O_3(10\bar{1}2)$ surface has been investigated under UHV conditions. The products are ethylene gas, ethane gas, hydrogen gas and adsorbed iodine. Thermal desorption experiments reveal two ethylene desorption features. The lower energy feature is desorption-limited while the higher energy feature is reaction-limited (Ea=151 kJ/mol). Similarly, two desorption features are observed for product ethane. The lower energy feature is desorption-limited, while the higher energy feature is reaction-limited. High temperature products share the same rate-limited step: β-hydride elimination from surface ethyl fragments. This reaction pathway is similar to that observed from the ethyl chloride reactant in Chapter 2.

The deposition of iodine leads to deactivation of the surface due to site blocking of surface Cr cations. No evidence is seen for the replacement of surface lattice oxygen by iodine because no oxygen contained desorption species are detected. No carbon is detected on the deactivated surface, indicating that decomposition to coke is not a significant reaction pathway for ethyl fragments under the conditions of the study.

3.6 References

[1] B.E. Bent, *Chem. Rev.* **96** (1996) 1361.

[2] B.E. Bent, R.G. Nuzzo, B.R. Zegarski and L.H. Dubois, *J. Am. Chem. Soc.* **113** (1991) 1137.

[3] I. Kovacs and F. Solymosi, *J. Phys. Chem.* **97** (1993) 11056.

[4] S. Tjandra and F. Zaera, *Surface Science*, **289** (1993) 255.

[5] G. Karamullaoglu, S. Onen and T. Dogu, *Chem. Eng. Proc.* **41** (2002) 337.

[6] P.M. Michalakos, M.C. Kung and I. Jahan, H. Kung, *J. Catal*. **140** (1993) 226.

[7] F. Zaera, *Surface Science*, **219** (1989) 453.

[8] M.X. Yang, S.K. Jo, A. Paul, L. Avila, B.E. Bent and K. Nishikida, *Surface Science*, **325** (1995) 102.

[9] A. Paul, M.X. Yang and B.E. Bent, *Surface Science*, **297** (1993) 327.

[10] X.L. Zhou, F. Solymosi, P.M. Blass, K.C. Cannon and J.M. White, *Surface Science*, **219** (1989) 294.

[11] The ion gauge sensitivity factor for ethyl iodide was estimated as 10.8 using the correlation by S. George reported in Brainard and R.J. Madix, *J. Am. Chem. Soc.*, **111** (1989) 3826.

[12] Mass spectrometer sensitivity factors for Ethyl iodide (m/z 29), ethylene (m/z 27), ethane (m/z 30) and dihydrogen (m/z 2) were 1.60, 0.68, 0.27 and 1.04, respectively.

[13] J.L. Lin and B.E. Bent, *J. Phys. Chem.* **96** (1992) 8529.

[14] J.F. Moulder, W.F. Stickle, P.E. Sobol, K.D. Bomben, J. Chastain (edited), Handbook of X-ray Photoelectron Spectroscopy, Perkin-Elmer Corporation, Eden Prairie, MN, 1992.

[15]M.A. Minton, Q. Ma and D.F. Cox, in preparation.

Chapter 4

Recommendations for Future Work

4.1 Recommendations for Future Work

XPS of ethyl iodide on the Cr_2O_3 $(10\bar{1}2)$ surface has already been reported in Chapter 3. The results demonstrate the ethyl iodide begins to dissociate below 200 K on the Cr_2O_3 $(10\bar{1}2)$ surface leaving iodine adatoms and a variety of surface hydrocarbon species. Similar experiments have not yet been performed on ethyl chloride to establish the temperature range associated with the initial dissociation process. XPS of ethyl chloride should be conducted to verify if the dissociation temperature is correlated to the gas phase C-X bond strength. Also, since the reaction products from ethyl chloride evolve in only one reaction limited temperature range, it should be possible to obtain a more definitive C 1s XPS spectrum for surface ethyl fragments.

Isotopic labeling experiments with partially deuterated ethyl iodide molecules (CD_3CH_2I) could provide additional support for the proposed reaction pathways. Using CD_3CH_2I could verify that the ethyl fragments undergo β-hydride elimination on Cr_2O_3 $(10\bar{1}2)$ if D_2 desorption (but no H_2 or HD) is observed in thermal desorption experiments. Such experiments have been performed on Pt (111) and Ni (100) [1,2], and show that nickel is selective for β-hydride elimination almost exclusively over other processes such as α-elimination, H-D exchange, insertion and coupling reactions. While on the Pt (111) surface, both β-hydride elimination and H-D exchange are observed.

1-bromo-1-chloroethane (Lancaster, 98%), 1,2-diiodoethane (Aldrich, 99%) and 1,1,1-trichloroethane (Aldrich, 99.5%) can be used to elucidate how the degree of halogenation of ethane effects the reaction mechanism under UHV system. For example, 1-bromo-1-chloroethane dehalogenation to surface ethylidene is expected. Testing different hydrocarbon surface fragments should give information on the reaction intermediates most closely associated with coke (surface carbon) formation.

4.2 References

[1] S. Tjandra, F. Zaera, *Surface Science*, **289** (1993) 255.

[2] F. Zaera, *J. Phys. Chem.* **94** (1990) 8350.